




CANFIS based DSTATCOM modelling for solving power quality problems

B. B. Bukata ^{a,*}, R. A. Gezawa^b

^a Department of Electrical Engineering, Bayero University Kano, Nigeria

^b Kano Electricity Distribution Company, KEDCO, Nigeria

ARTICLE INFO

Article history:

Received 4 February 2021

Received in revised form
6 March 2021

Accepted 7 March 2021

Available online
18 March 2021

Keywords:

ANFIS

CANFIS

DSTATCOM

Power quality

Smart grid

ABSTRACT

Devolution of the power grid into smart grid was necessitated by the proliferation of sensitive load profiles into the system, as well as incessant environmental challenges. These two factors culminated into aggravated disturbances that cause serious havoc along the entire system structure. The traditional proportional-plus-integral-plus-derivative (PID) solution offered by the distribution synchronous compensator (DSTATCOM) could no longer hold. As such, this paper proposes some soft-computing framework for redesigning DSTATCOM to automatically deal with power quality (PQ) problems in smart distribution grids. A recipe of artificial neural network (ANN) and coactive neuro-fuzzy inference systems (CANFIS) was fabricated for the objective. The system was modelled, simulated, and validated in MATLAB/Simulink SimPowerSystems environment. The performance of the CANFIS against adaptive neuro-fuzzy inference systems (ANFIS), ANN and fuzzy logic controllers' algorithms proved superior in handling PQ issues like voltage sag, voltage swell and harmonics.

1. Introduction

Researchers have recently shown ardent interest in exploring the control problem in smart grid, and proffered new solutions. A document recently prepared by the IEEE Control System Society captioned "Smart Grid Vision", presents concepts in control strategies that would meet the challenges of this future power grid [1]. Conversely, rapid decentralisation of the energy mix involving distributed energy resources in the form of renewable energy sources (RES) such as solar photovoltaic (PV) and rooftop farms, wind farms, and energy storage systems, was least expected by the energy experts.

However, both real-world complex problems presented by the integration of RES

into the main grid and two-way communication backbones involved in a smart grid design require intelligent solutions from diverse sources. Hence, soft computing as a ground-breaking approach in creating computational intelligent systems comes to mind [2]. When accomplished, the intelligent solutions should be able to learn and mimic human expertise, and also be able to robustly adapt to changing environments to appropriately deal with power quality (PQ) problems.

A PQ problem has often been expressed in relation to the deformations in sinusoidal waveforms of load currents or supply voltages given at fundamental frequency, whose amplitude is the same as the rated root mean square (rms) value in a three-phase system

* Corresponding author

E-mail address: boyibukata@yahoo.com

<https://doi.org/10.37121/jase.v4i2.148>

[3]. These deformations result in establishing PQ issues such as voltage sags, voltage swells, harmonics and inter-harmonics of the fundamental waves that can trigger serious deviations in system's normal behaviour.

According to IEEE Std. 1159 (1995), sag and swell magnitudes range from 10 – 90 %; 110 – 180 % of nominal voltage and sag durations from half cycle to 1 min, respectively [4], [5]. Voltage sags represent the commonest PQ issues to industrial and large commercial customers in damaging sensitive equipment, leading to losses in daily productions and finances. Some of the sensitive equipment include adjustable speed drives (ASDs), chiller controllers, and programmable logic controllers (PLCs). Sags, swells and harmonics are some of the PQ problems solvable through distribution synchronous compensator (DSTATCOM). Moreover, sags may be classified according to their duration as presented in Table 1 [6].

Table 1 Classification of voltage sag according to IEEE [4].

Type of Sag	Duration	Magnitude
Instantaneous	0.5 – 30 cycles	0.1 – 0.9 p.u.
Momentary	30 cycles – 3 s	0.1 – 0.9 p.u.
Temporary	3 s – 1 min	0.1 – 0.9 p.u.

The DSTATCOM is a shunt device belonging to the Flexible ac transmission systems (FACTS) family. It may be configured with IGBT switches having frequency range of 2 – 4 kHz, a coupling transformer, a dc capacitor link, and an external controller as illustrated in Fig. 1 [3]. The traditional proportional-plus-integral (PI) controller seen in the figure would subsequently be replaced by the proposed CANFIS scheme.

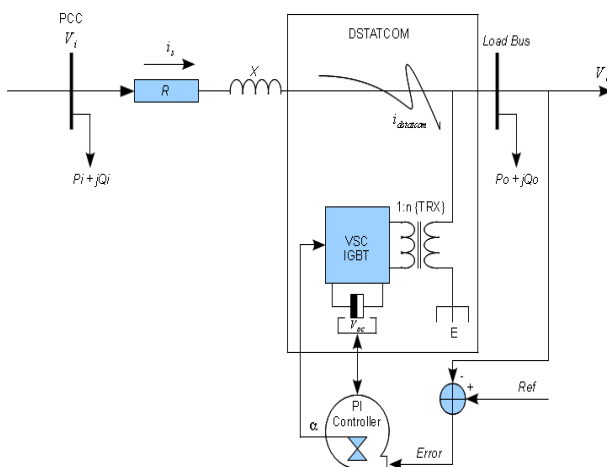


Fig. 1 Shunt DSTATCOM with a PI controller [3]

Fig. 2 presents a coactive neuro-fuzzy inference (CANFIS) mechanism proposed in this paper, and as originally presented by [6]. It spans across the two extremes of the neuro-fuzzy (NF) spectrum, characterised by a black-box ANN and a fuzzy inference system (FIS). Moreover, the scheme is an extension of the adaptive neuro-fuzzy inference systems (ANFIS) used to solve PQ problems via unified power quality conditioner (UPQC) in [2]. This technique was verified to produce remarkable results in the control of voltage sags and harmonic contents [7].

The fact that ANFIS has the ability to use its hybrid nature to learn and strategically tune Tagaki-Sugeno-Kang (TSK) FIS, makes its CANFIS extension even more appropriate for solving complex problems. Based on this philosophy, this paper applies CANFIS in DSTATCOM for the control of PQ issues such as voltage sags, voltage swells, and harmonics reduction. Many other applications based on similar models have also been seen in the literature [8]. The ensuing NF models can then be defined by the NF spectrum with respect to linguistic precision for input-output mappings [9].

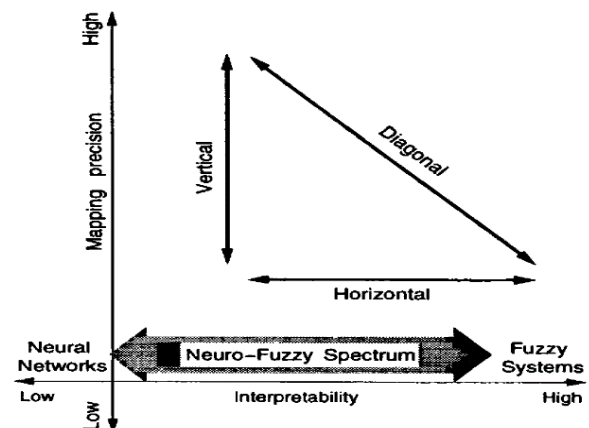


Fig. 2 Neuro Fuzzy Spectrum [2].

Fig. 2 illustrates the concept of NF spectrum regarding the trade-offs involved in fuzzy inferencing procedure depicted on the horizontal route, while the input-output precision mapping is shown on the vertical route. This way, the control rate of the DSTATCOM will get updated automatically each time a new rule is learnt by the neural networks and admitted for firing by the FIS, giving rise to tight control regimes perfect for taming PQ issues. Modelling, simulation, and validation of this work were carried-out in SimPowerSystems environment. The results obtained were superior as compared with the ANFIS based UPQC.

The remainder of the paper is organised as follows: Section two presents the materials and methods used in implementing the technique. Section three discusses the results obtained. Section four draws conclusion on the paper, followed by the references.

2. Materials and Methods

2.1. Design of DSTATCOM

Essentially, this voltage source converter generates controllable ac voltage source from the stored energy in the dc capacitor link that appears behind the coupling reactance. Since the dc energy storage is shallow, it is thus not possible to exchange real power with the network. Nevertheless, the reactive power exchange is realised by either injecting or absorbing reactive current at the point of common coupling (PCC) through the coupling reactance. Consequently, the DSTATCOM can operate as an inductor when $|V_i| < |V_o|$ or a capacitor when $|V_i| > |V_o|$. However, there is no DSTATCOM action needed in a steady state operation for $|V_i| = |V_o|$ [3]. For example, V_i and V_o are in equation (1).

Advantages of DSTATCOM:

- The DSTATCOM is capable of injecting reactive current.
- It has a quick response time in the range of 8 – 30 ms, which makes it suitable to compensate negative currents, as well as minimise flicker.
- It is possible to control active power and maintain system stability with the DC energy storage circuit in DSTATCOM.
- DSTATCOM requires smaller footprint for installation.
- The DSTATCOM is a shunt device, capable of generating and/or absorbing controllable reactive power.

DSTATCOM model from Park's transformation: Fig. 3 shows the equivalent circuit of DSTATCOM. Power exchange (absorption or injection) at the PCC is a function of the model's accuracy. But for online control requirements, application of the nonlinear model is made to represent the most practical system's nonlinearities, as well as to isolate any involvement of linear model approximations responsible for creating modelling errors between the models [3]. The mathematical expressions relating the system current (I), real power (P), reactive power (Q), and the power or load angle (φ) to the system voltages utilised for this study are given as:

$$I = \frac{V_i - V_o}{jX} \quad (1)$$

$$P = \frac{V_i V_o}{X} \sin \varphi \quad (2)$$

$$Q = \frac{V_i V_o}{X} \cos \varphi \quad (3)$$

where V_i is the input source bus voltage, V_o is the DSTATCOM output bus voltage, X the system reactance, and φ is the power or load angle between the input and output bus voltages measured in degrees.

The dynamic equations governing the instantaneous values of the three-phase voltages across the two sides of DSTATCOM were fully described in [6]. However, the well-known Park's transform leading to the modelling of the equivalent system from the sending end through the receiving end, obtained from the following relations (4), is characterised by equation (5):

$$\left(R_p + L_p \frac{d}{dt}\right) i_p = V_t V_p \quad (4)$$

Where, R_p and L_p are the parallel resistance and inductance of the DSTATCOM, i_p and V_t are the absorbed/injected DSTATCOM current and coupling transformer voltage, respectively; given that:

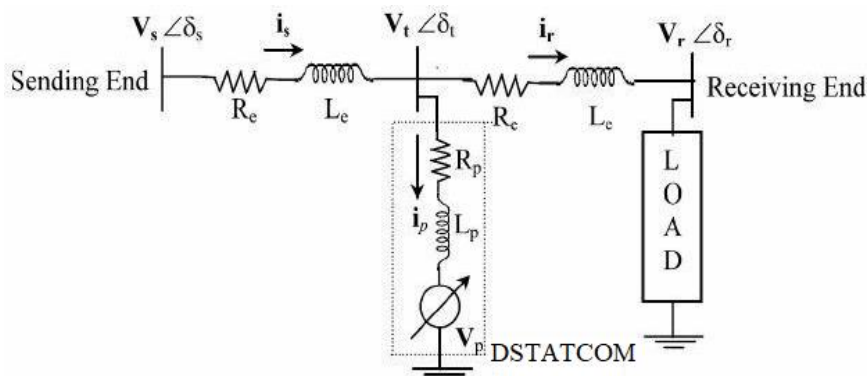


Fig. 3 Equivalent circuit of system with DSTATCOM [6].

$$i_p = (i_a \ i_b \ i_c)^T; \quad V_t = (V_{ta} \ V_{tb} \ V_{tc})^T; \quad \text{and} \\ V_p = (V_{pa} \ V_{pb} \ V_{pc})^T.$$

$$T = \frac{2}{3} \begin{pmatrix} \cos \theta & \cos\left(\theta - \frac{2\pi}{3}\right) & \cos\left(\theta + \frac{2\pi}{3}\right) \\ -\sin \theta & -\sin\left(\theta - \frac{2\pi}{3}\right) & -\sin\left(\theta + \frac{2\pi}{3}\right) \\ \frac{1}{\sqrt{2}} & \frac{1}{\sqrt{2}} & \frac{1}{\sqrt{2}} \end{pmatrix} \quad (5)$$

Passing through the dq0 transform, the new two-phase equations derived are given as equation (6); where, V_d , V_q , V_0 ; i_d , i_q , i_0 ; and V_a , V_b , V_c ; i_a , i_b , i_c are the direct, quadrature, and zero sequence, as well as three-phase voltages and current components. T is the factor of park's transform from pq0 plane to abc three-phase sequence.

$$\begin{pmatrix} V_d \\ V_q \\ V_0 \end{pmatrix} = T \begin{pmatrix} V_a \\ V_b \\ V_c \end{pmatrix} \quad \begin{pmatrix} i_d \\ i_q \\ i_0 \end{pmatrix} = T \begin{pmatrix} i_a \\ i_b \\ i_c \end{pmatrix} \quad (6)$$

Thus, the dynamic DSTATCOM model can be described simultaneously by equations (7) to (8) as:

$$\frac{di_{pd}}{dt} = -\frac{R_p}{L_p} i_{pd} + \omega i_{pq} + \frac{1}{L_p} (V_{id} - V_{pd}) \quad (7)$$

$$\frac{di_{pq}}{dt} = -\frac{R_p}{L_p} i_{pq} - \omega i_{pd} + \frac{1}{L_p} (V_{iq} - V_{pq}) \quad (8)$$

Where, $\omega = (d\theta/dt)$, is the source angular velocity.

Details of voltage control strategy for DSTATCOM and its objectives can be found in [3], [6], [10], [11]. Table 2 presents the list of all the parameters used for the DSTATCOM design and other simulation exercises.

Table 2 DSTATCOM plant parameters [3].

Parameter	Values
Frequency (f)	50 Hz
Resistance (R)	1 Ω
Capacitance (C)	550 μF
Inductance (L)	3 mH
Total reactance ($jX = X_o + X_i$)	5.13 Ω
Feeder ac-voltage (V)	415/220 V
Modulation-index (m)	1
Angular-frequency (ω)	377 rad/s
Switching-angle (α)	$\pm 30^\circ$ (± 0.5326) rad
Reactive-current (i_q)	38 A
Direct-current (i_d)	0.2 A
Capacitor-link dc-voltage (V_{dc})	380 V

2.2. CANFIS Architectural Design

Framework of the CANFIS has been described by [9] in terms of a radial basis

function network (RBFN) and the back-propagation multilayer perceptron (MLP). However, its extension is made possible through a single output ANFIS scheme to produce multiple outputs [2]. One approach of achieving this is by placing several ANFIS models in parallel to match the number of required outputs. But, two major concerns are imminent:

- modifiable parameters cannot be shared as each ANFIS model has independent set of fuzzy rules that make it hard to correlate between outputs; and
- adjustable parameters tend to hugely increase with increasing outputs.

In order to remedy these concerns, the CANFIS and RBFN architecture considers a locality phenomenon by Euclidean norms between each local centre and the output vector as demonstrated in Fig. 4. The single output ANFIS/CANFIS schemes are illustrated in Figs. 4(a-d). Once the three (input, hidden, and output) neurons acquire identity functions as in Fig. 4d, then CANFIS assumes the characteristics of a TSK fuzzy inference depicted in Fig. 4a, which accomplishes the following linear fuzzy *if – then* rules:

Rule 1:

$$\text{If } x \text{ is } A_1 \text{ and } y \text{ is } B_1, \text{ then } C_1 = p_1x + q_1y + r_1 \quad (9)$$

Similarly, by applying a nonlinear rule, the functionality and performance of any adaptive network can be extended. The chosen activation function should impose no constraints on its boundary, and will produce a nonlinear consequent C_1 . In this case, a sigmoid function of the following form is chosen:

$$C_1 = \frac{1}{1 + \exp[-(p_1X + q_1Y + r_1)]} \quad (10)$$

Fig. 4e presents the consequent parts namely, C_1 and C_2 as symbolised in a layered network depiction for making clearer comparison with the back-propagation MLP mentioned above. From the ongoing, it is noted that CANFIS derives its power from the weights existing between the consequent layer and the fuzzy inference layer, which solely depends on patterns. And the membership function values generated would correspond to those changeable weights that are input-pattern dependent. Hence, CANFIS can be locally tuned in the same manner as the RBFN to give accurate results. The reader is further referred to [2] and [6] for implementation details.

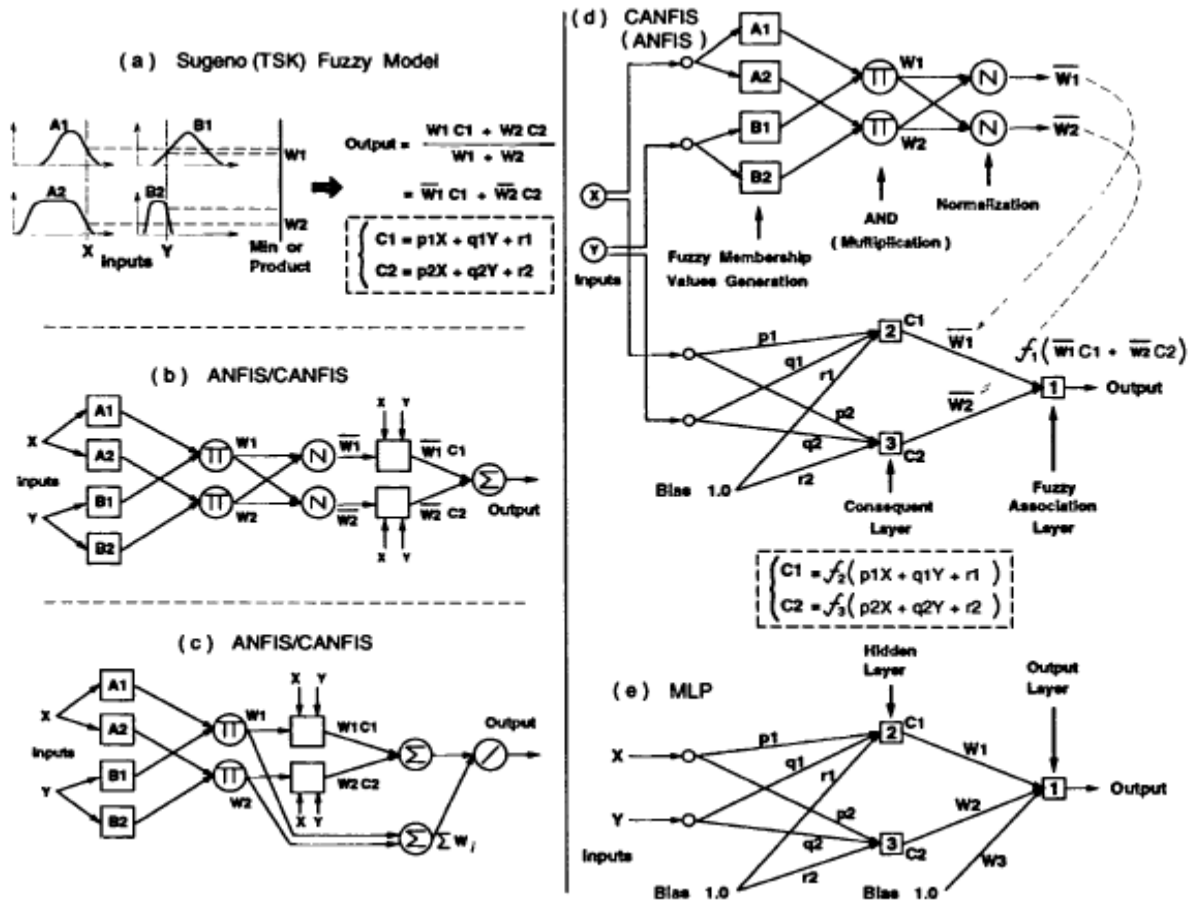


Fig. 4 (a) A two input, one output TSK fuzzy model; (b-d) Equivalent ANFIS/CANFIS architectures; (e) A simple comparable back-propagation MLP [2].

3. Results and Discussion

3.1. The CANFIS/DSTATCOM Truth Model

In this section, a truth CANFIS based DSTATCOM model is developed and simulated in SimPowerSystems software as shown in Fig. 5. A number of simulations were conducted to verify the effectiveness of the technique against its ANFIS counterpart which was developed for UPQC according to the list of parameters given in Table 2.

3.1.1 Sag conditions: It is seen from section 2 that to satisfy voltage sag and voltage swell, a decrease of 0.1–0.9, or an increase of 1.1–1.8 per-unit rms values within the range from 1ms to 1 min must be attained. The model in Fig. 5 was used for this study. A sag-laden distant load situated at the consumer's premises was first simulated to create a sag condition. Connecting an inductive load in series with a three-phase circuit being excited by a sinusoidal input, the direct-online (DOL) starter draws a heavy current shown inset of Fig. 6, thereby initiating the sag. A closer look at Fig. 6 shows

the little variation in the current responsible for causing the sag between 0.4 - 0.5 s. Hence, the deployment of CANFIS equipped DSTATCOM is required to minimise sag strength. The steady state responses at PCC for both reactive (blue) and active (red) powers during sag condition are shown in Figs. 7 and 8.

3.1.2 Swell condition: Equally, a swell condition is created by connecting another distant load in parallel as shown in Fig. 9. A swell, which is the reverse of sag, is triggered by causes such as sudden drops in large load, high-impedance neutral connections and a single-phase fault on a three-phase system. The penalty for such irregularity can range from flawed data to electrical contact erosion, as well as damage to sensitive semiconductor devices [3]. A closer look of the swell (overvoltage) condition is clearly shown to occur as usual between 0.4 and 0.5 s, before the DSTATCOM is brought into operation. A current rush of 0.125 A magnitude responsible for the swell is noticed almost doubling its original value (0.067 A), i.e., an increase of 50%.



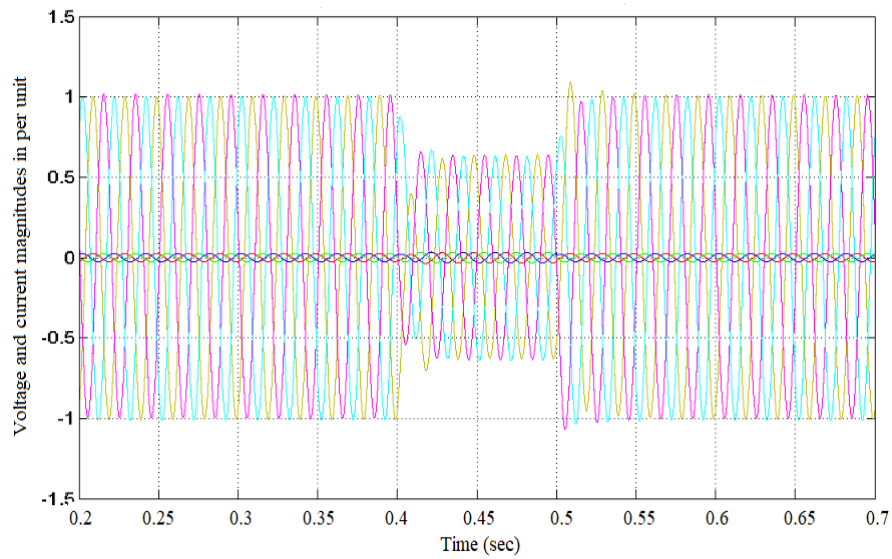


Fig. 6 Voltage at 0.6 per-unit decrease.

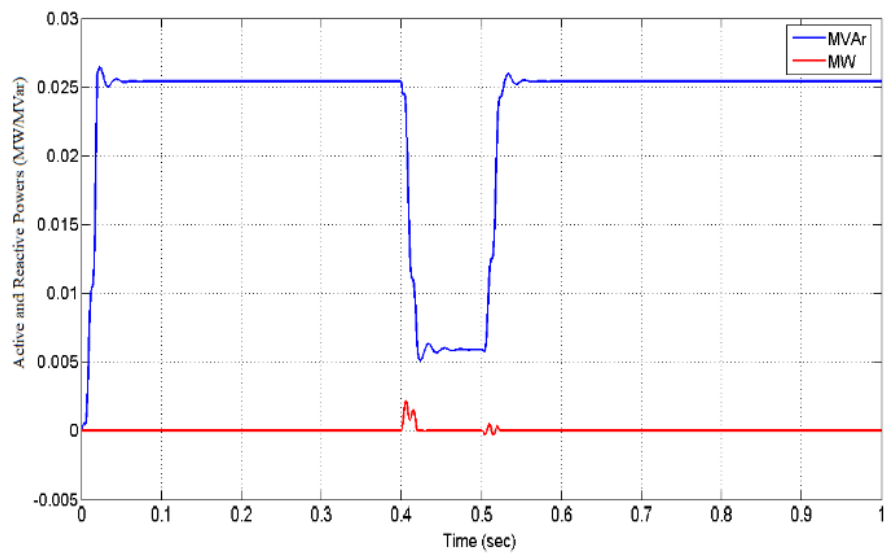


Fig. 7 Step response on MW/MVar sag.

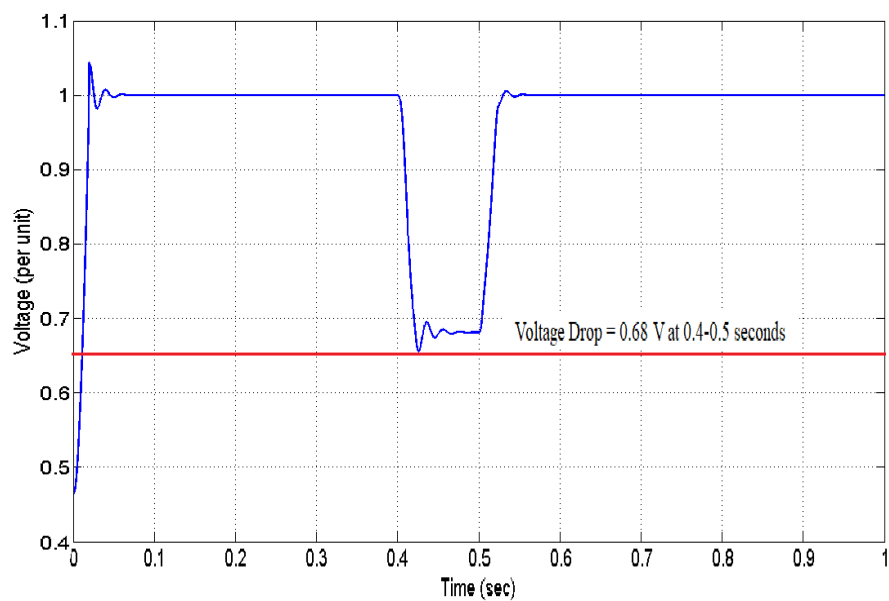


Fig. 8 Step response voltage sag.

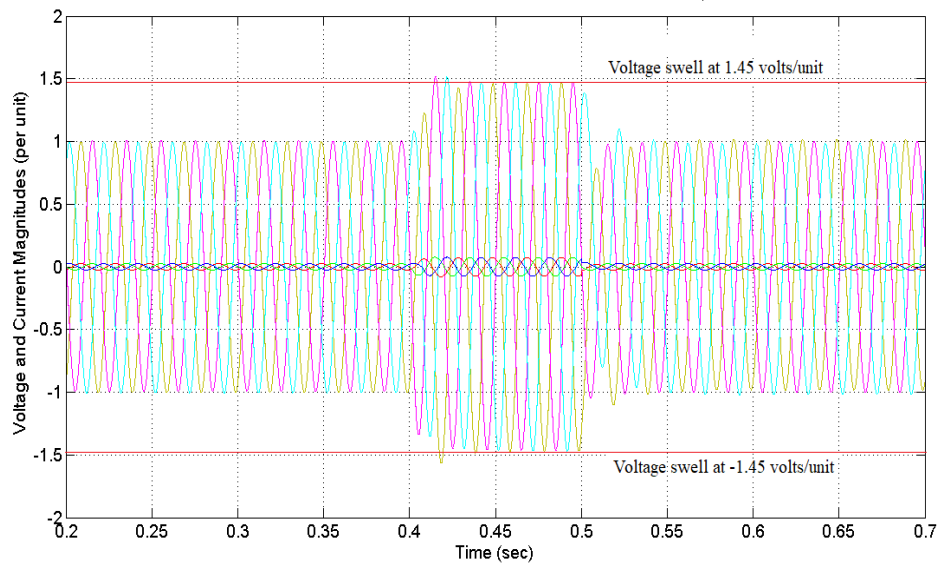


Fig. 9 Three-phase voltage swells.

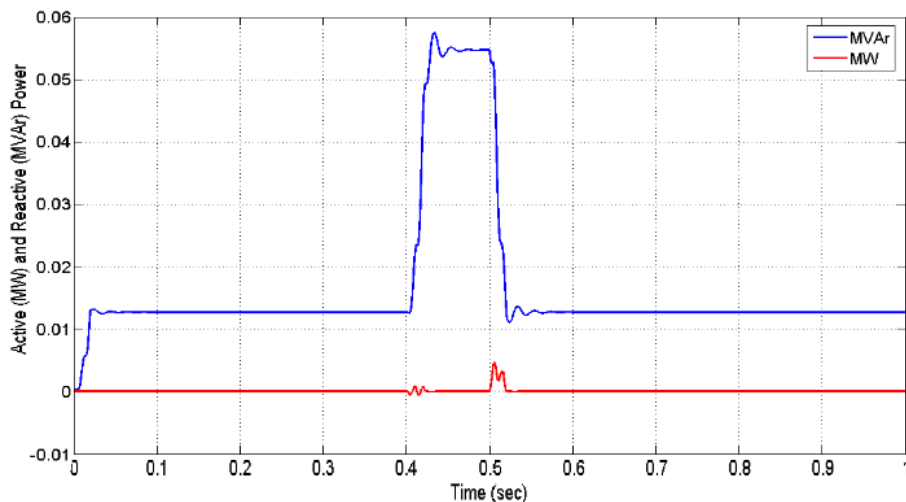


Fig. 10 Step response on MW/MVar swells.

The power exchanges involved during the swell condition reversed the anomalies of the active component shown in Fig. 10. Also, the amount of reactive power demand caused by the current rush can be seen shooting from its nominal 0.013 MVar to 0.055 MVar at the end of the swell. The voltage rise due to the sag is shown in Fig. 11, where an increase in PCC voltage is raised to 46 % of its nominal per-unit value during the scenario.

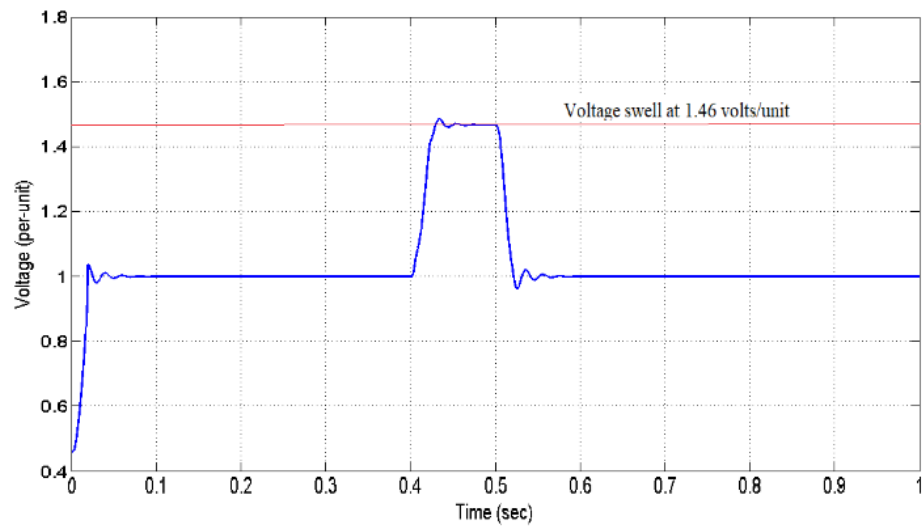
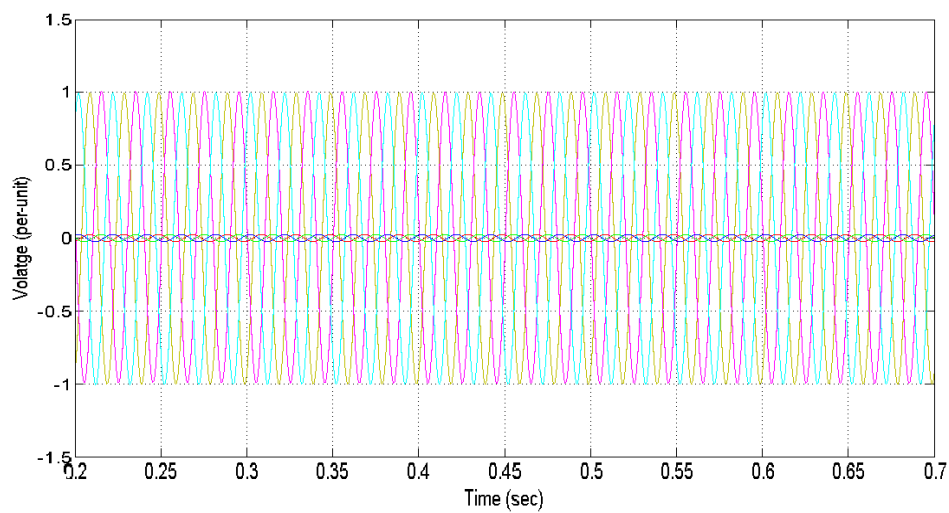
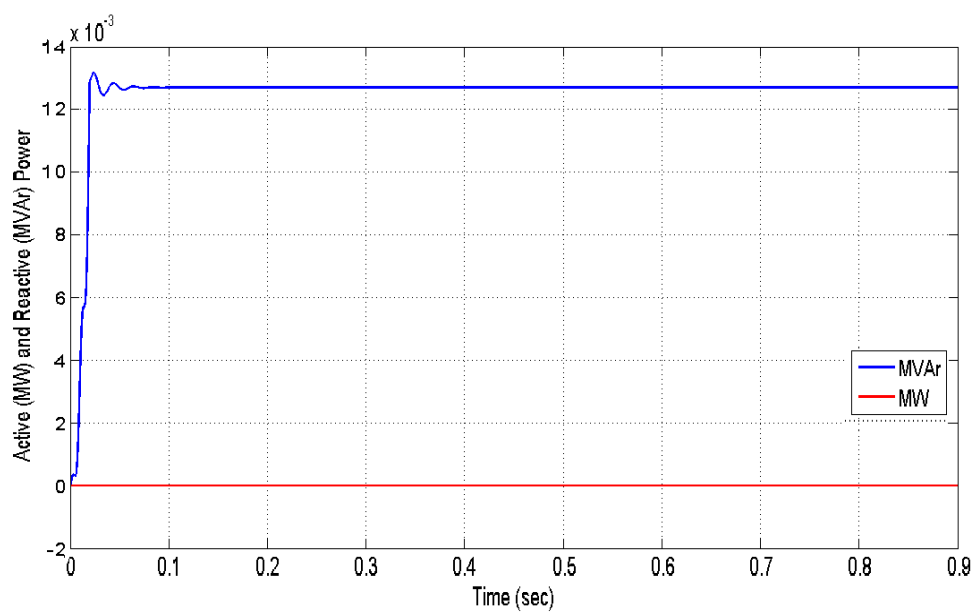
3.1.3 Intervention of CANFIS DSTATCOM: The proposed CANFIS is now deployed into the circuit and operation subsequently evaluated. The no fault voltage and current quantities can immediately be observed in Fig. 12, in which the sag and the swell had for once been mitigated CANFIS.

Both Figs. 13 and 14 also depict the step responses to active and reactive powers, in addition to the no-load voltage at the PCC,

respectively. The active power is maintained at zero, while the reactive power reaches its maximum value of 0.0128 MVar for unit input signals.

The current injected by the CANFIS during the sag condition is shown in Fig. 15. The current surge generated in tackling the deficiency at 0.4 – 0.5 s, before restoring normal operations.

3.1.4 Harmonics control: This section looks into the efficacy of our CANFIS technique to harmonics current elimination. Comparison was later made with other control techniques in Table 3 in order of superiority. It is vividly seen from the table that all the methods have met the provision made by IEEE Std. 519 - 1992 for maintaining total harmonic distortion (THD) within 5%. But, CANFIS produced the best result with 0.00% harmonics.

**Fig. 11** Step response voltage swell.**Fig. 12** Mitigated three – phase voltages.**Fig. 13** Mitigated MW/MVar step response.

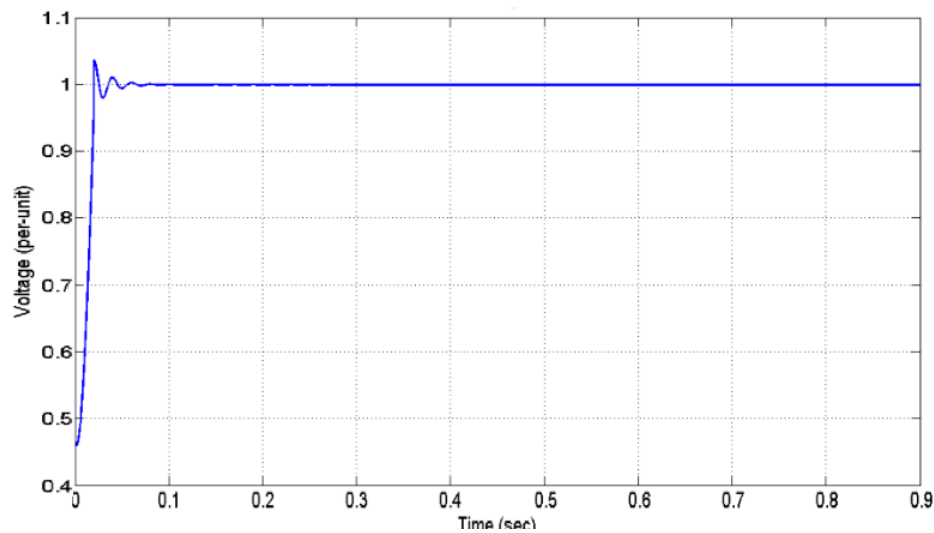


Fig. 14 Mitigated voltage step response.

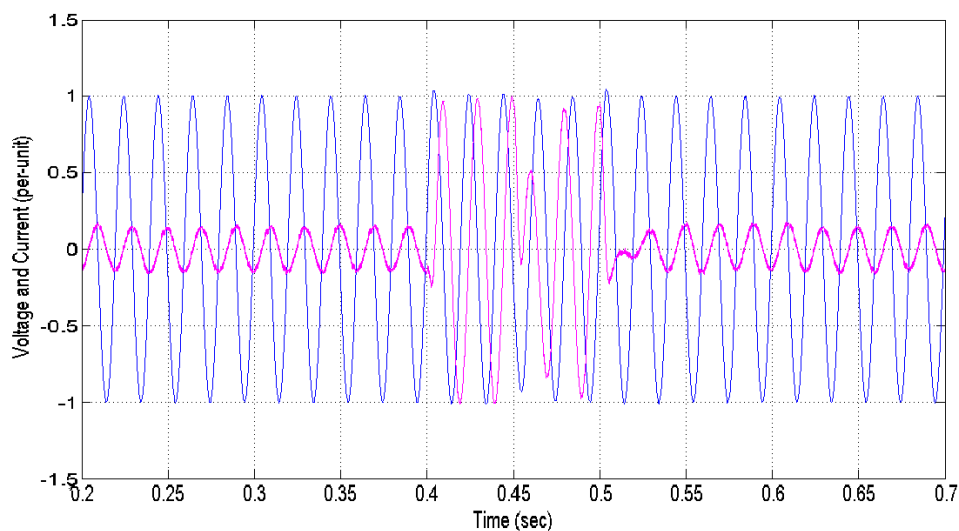


Fig. 15 Reactive current injected at PCC (maroon).

Table 3 Comparing harmonics reduction.

Regime	THD Reduction (%)	Remarks
CANFIS	0.00	Best
ANFIS	0.42	Satisfactory
ANN	0.85	Satisfactory
FLC	0.96	Satisfactory

The bar charts in Figs. 16 to 19 graphically depicted the contribution made by each method namely, CANFIS, ANFIS, ANN, and FLC.

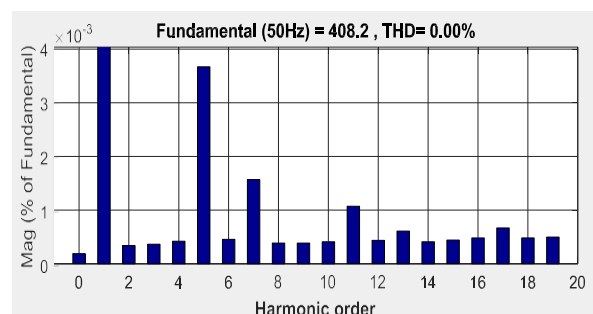


Fig. 16 CANFIS Controlled DSTATCOM.

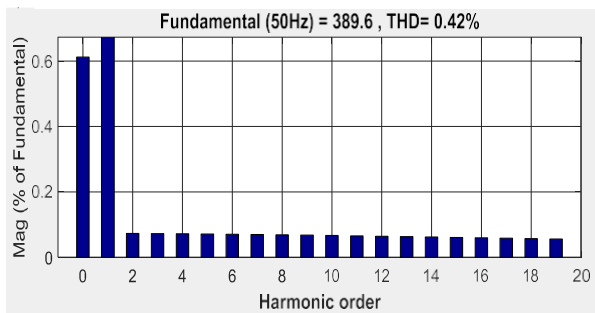


Fig. 17 ANFIS Controlled UPQC.

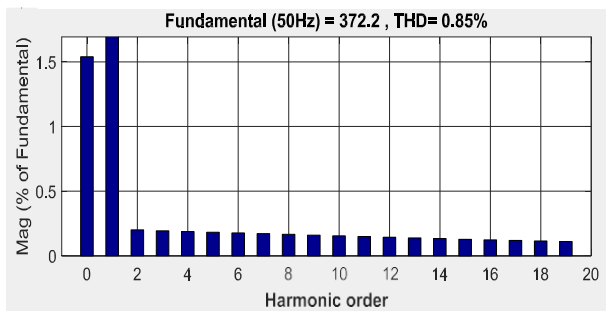


Fig. 18 ANN Controlled DSTATCOM.

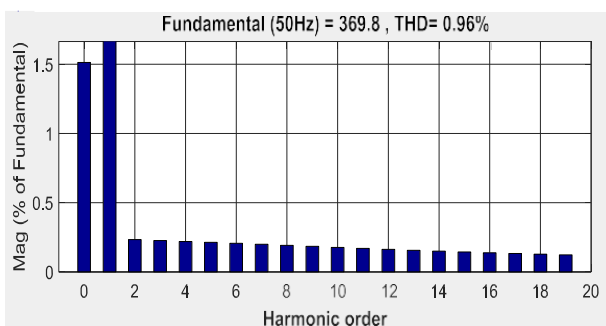


Fig. 19 FLC Controlled DSTATCOM.

4. Conclusion

This paper presented the extended CANFIS version of ANFIS applied to DSTATCOM control of PQ problems. Voltage sag and swell conditions were simulated with and without the CANFIS and the results showed remarkable improvement in the control of these deformations. Further tests on Total Harmonic Voltage Distortion (THDv) also attested to the superiority of the new method giving a THDv reduction of 0.00%, by far better than the 0.42%, 0.85%, and 0.96% contributed by ANFIS, ANN, and FLC, respectively, while satisfying the stipulated by IEEE Std. 519 – 1992 for maintaining 5% THDv.

Conflict of Interests

The authors declare that there is no conflict of interests regarding the publication of this paper.

ORCID

B. B. Bukata  <https://orcid.org/0000-0002-2841-4710>

References

- [1] J. Stoustrup, A. Annaswamy, A. Chakraborty, and Z. Qu, (Eds.), "Smart grid control: overview and research opportunities," Switzerland: Springer Cham, 2019; doi: 10.1007/978-3-319-98310-3
- [2] J-S. R. Jang, C-T. Sun, and E. Mizutani, "Neuro-fuzzy and soft computing: A computational approach to learning and machine intelligence," NJ: Practice Hill, 2007.
- [3] B. B. Bukata, "Evolutionary optimisation for volt-var power quality control," Ph.D. Thesis, University of Glasgow, 2012.
- [4] IEEE recommended practices and requirements for harmonic control in electric power systems, 1993.
- [5] Chapman. Power quality and utilisation guide section 5 - introduction, November 2001 <http://www.copperinfo.co.uk/powerquality/downloads/pqug/51-voltage-dips.pdf>
- [6] M. Paul, and P. R. Kasar, "Voltage sag mitigation by D-STATCOM using voltage regulation technique," *Int. Journal of Engineering Research & Technology*, vol. 3 no. 5, pp. 96-101, 2014.
- [7] B. B. Bukata and R. A. Gezawa, "Design of an efficient ANFIS based UPQC harmonics control in electrical power system," *Proceedings of 2nd Int. Conference on Green Engineering for Sustainable Development*, Bayero University Kano, Nigeria, 2017, pp. 65 – 71.
- [8] E. Mizutani, J-S. R. Jang, K. Nishio, H. Takagi and D. M. Anslander, "Coactive neuro-fuzzy modelling for colour recipe prediction," *Proceedings of ICNN'95 – Int. Conference on Neural Networks*, Perth, WA, Australia, 1995, pp. 2252-2257.
- [9] E. Mizutani and J-S. R. Jang, "Coactive neuro-fuzzy modelling," *Proceedings of Int. Conference on Neural Networks*, Perth, WA, Australia, November 27 - December 1, 1995, pp. 760 – 765.
- [10] W. Freitas, E. Asada, A. Morelato, and Wilsun Xu, "Dynamic improvement of induction generators connected to distribution systems using a DSTATCOM," *Proceedings of Int. Conference on Power System Technology*, Kunming, China, 2002, pp. 173-177.
- [11] N. G. Hingorani and L. Gyugyi, "Understanding FACTS: Concepts and technology of flexible ac transmission systems", NY: Wiley-IEEE Press, 1999.
- [12] T. Tagaki and M. Sugeno, "Fuzzy identification of systems and its application to modelling and control," *IEEE Transactions on Systems, Man, and Cybernetics*, vol. SMC-15, no. 1, pp. 116 – 132, 1985.